water

MDPI

Article

Simulation of Runoff through Improved Precipitation: The Case of Yamzho Yumco Lake in the Tibetan Plateau

Handuo Tang [1,2], Fan Zhang [1,2], Chen Zeng [1,*], Li Wang [1], Hongbo Zhang [3], Yuxuan Xiang [1,2] and Zhongbo Yu [4]

1 State Key Laboratory of Tibetan Plateau Earth System, Environment and Resources (TPESER), Institute of Tibetan Plateau Research, Chinese Academy of Sciences, Beijing 100101, China
2 University of Chinese Academy of Sciences, Beijing 100049, China
3 College of Water Resources & Civil Engineering, China Agricultural University, Beijing 100107, China
4 State Key Laboratory of Hydrology-Water Resources and Hydraulic Engineering, Hohai University, Nanjing 210098, China
* Correspondence: zengchen@itpcas.ac.cn

Abstract: Alpine lakes on the Tibetan Plateau have significantly changed under a changing climate over past decades. However, the changing patterns of the inflow sources of the lakes, i.e., rainfall and the melt water of snow and glaciers, and their response to climate change remain uncertain because obtaining accurate precipitation and melt water discharge is difficult due to the complex topography, spatial variability, and scarce stations of the alpine area. A distributed hydrological model, J2000, was employed in this study to simulate runoff component variations of the Yamzho Yumco Lake glaciated basin during 1974–2019. Except for observed daily runoff from two tributaries, a High Asia Refined (HAR) high-resolution reanalysis of precipitation data was combined with field precipitation gradient observation and snow cover area validation, all performed simultaneously to reduce the uncertainty of inflow components in the model. Results showed that the average runoff into the lake during 1974–2019 was $5.5 \pm 1.4 \times 10^8$ m^3/10a, whereas rainfall runoff, glacier melt runoff, snowmelt runoff, and baseflow contributed to 54.6%, 10.8%, 1.8%, and 32.7% of total runoff in mean, respectively. Seasonal runoff in spring, summer, autumn, and winter accounted for 6.7%, 60.6%, 23.9% and 8.8% of annual total runoff, respectively. In glacial areas, the reduction in total runoff after removing the precipitation trend was 1.4 times than that of temperature, and in non-glacial areas, the reduction in total runoff after removing the precipitation trend was 1.6 times than the increase in total runoff after removing the temperature trend. The proportion of rainfall runoff increased at a rate of 1.0%/10a, whereas the proportion of melt runoff decreased at a rate of 0.07%/10a during the study period.

Keywords: glaciated basin; runoff components; hydrological model; Yamzho Yumco Lake; Tibetan Plateau

check for updates

Citation: Tang, H.; Zhang, F.; Zeng, C.; Wang, L.; Zhang, H.; Xiang, Y.; Yu, Z. Simulation of Runoff through Improved Precipitation: The Case of Yamzho Yumco Lake in the Tibetan Plateau. *Water* **2023**, *15*, 490. https://doi.org/10.3390/w15030490

Academic Editors: Yaoming Ma, Binbin Wang, Jiming Jin and Lijuan Wen

Received: 29 November 2022
Revised: 18 January 2023
Accepted: 24 January 2023
Published: 26 January 2023

1. Introduction

Climate change has contributed to changes in the hydrological cycle in recent decades [1]. The glacial areas are sensitive to temperature, and the role of glacier melt to river runoff means that the hydrologies of these areas are sensitive to climate change [2]. The Tibetan Plateau (TP) holds many lakes and glaciers, due to which it acts as a storehouse for fresh water. These fresh water sources support one-sixth of the global population [2]. Climate warming has had a significant impact on TP by driving environmental change and water balance change, such as by reducing glaciers and snow cover.

Multiple processes contribute to the hydrological process on the TP, including rainfall, glacier melt, and snowmelt [3,4]. Monthly distributions and inter-annual variations of runoff components, i.e., snowmelt and glacier melt, can affect total runoff and its distribution, which in turn can affect regional water resources and socioeconomic development [5–7]. The glacier melt runoff contribution to total runoff on the TP will increase due to a warming climate [8]. Lutz et al. [9] predicted increasing runoff from the

Indus River basin until 2050 due to increased glacier meltwater. A study of Central Asia by Kong et al. [10] identified increasing trends in river runoff recharge due to glacier melt runoff in recent years, with a positive relationship between the proportion of glacier melt runoff contribution to river recharge and the increase in total runoff. The dynamics of snow cover area (SCA) can affect the recharge mechanisms of major rivers in Asia significantly [11]. Climate warming has reduced the SCA; thus, it resulted in an earlier snowmelt runoff, an increased snowmelt period, and increased snowmelt runoff in winter and spring [12,13].

The TP is also known as a water tower, which means that water from runoff and lake in this region has large impacts on downstream water availability. Among the high-elevation plains on Earth, it has the highest average altitude and the largest area lakes, accounting for more than half of all lakes in China [14–16]. Because many lakes on the Tibetan Plateau are surrounded by glaciers, recharge to these lakes is mainly through rainfall, glacier melt, and snowmelt [17]. Because the alpine glaciers and inland lakes are sensitive to climate data such as temperature and precipitation, they could be used as indicators to reveal climate change processes [18]. Air temperature has significantly increased in recent years, which has driven the accelerated melting of glaciers throughout the plateau. This has in turn resulted in the expansion of alpine lakes supplied mainly by melt runoff [19,20]. Qiao et al. [21] found that the main driver that affected the alpine lakes' variability in the northwestern TP was glacier melt. In addition, many case studies have found that lake expansion was mainly affected by glacier melt runoff, such as in the Nam Co [22–24] and Selin Co [25–27]. Therefore, it is necessary to explore the response of alpine regions to surface runoff under climate change.

The Yamzho Yumco Lake falls in the Indian monsoon region in the southern TP [28]. The northern part of the lake basin is adjacent to the Yarlung Tsangpo River, separated only by 8–10 km at the closest point. There have been various studies on climate change's impact on the Yamzho Yumco Lake basin. Remote-sensing data of lake water levels obtained in recent years have shown that the Yamzho Yumco Lake was experiencing declining lake levels, whereas the other lakes' water levels on the TP were mostly increasing. Monitoring data for the lake confirmed declining lake levels during recent decades [29]. However, the correlation between lake water level and climate factors was the main study direction of previous studies [30]; another focus was using remote sensing imagines, satellite altimetry, and statistical analysis to identify the factors regulating changes to the Yamzho Yumco Lake [31–34]. The Yamzho Yumco Lake basin's complex terrain has limited available observations of runoff into the lake. Due to the complex terrain and limited observation data, previous studies used different methods to obtain inflow runoff into the lake, e.g., the stable isotope combined with water balance method [35], runoff coefficients [31], the water balance equation (runoff equals to precipitation minus evaporation) [36], and calculations of the difference between measurements of runoff (rainfall, snowmelt and glacier melt runoff) and simulated runoff (rainfall and snowmelt runoff) using the VIC model with a 0.25° resolution [37]. There has been increased attention towards the Yamzho Yumco Lake over the last few decades due to concern over its declining water levels. Among the driving data of the hydrological model, the precipitation data have the greatest impact and uncertainty. The spatial variability of precipitation increases with the increase of topographic effect [38,39]; some studies have shown that there were significant differences in precipitation even in a very small spatial range [40,41]. Many studies have compared the applicability of different precipitation products and found that the reanalysis precipitation data could provide a reference for large-scale precipitation research, but it would have rough resolution [42,43]. In the Tibetan Plateau, the downscaling of reanalysis data from High Asia Refined with higher resolution was applied to hydrometeorological research [44–46].

In this study, High Asia Refined (HAR) data combined with long-term field rainfall observations, which can provide an effective solution to the scarcity of precipitation data in the region, were employed to identify precipitation gradients of the study basin. The J2000 distributed hydrological model was used to simulate long-term runoff from the glacial and non-glacial areas of the Yamzho Yumco Lake basin. The novelty was to implement High Asia Refined (HAR) high-resolution reanalysis of precipitation data combined with field precipitation gradient observations as input, snow cover area validation, and calibration and validation of daily runoff observed from two tributaries to reduce the uncertainty of the model simulation. The specific objectives were to: (1) improve precipitation input in alpine lake basins based on reanalysis data; (2) reveal interannual and intra-annual changing patterns of surface runoff and its components into the Yamzho Yumco Lake; (3) identify responses of surface runoff into the lake to climate change. The present study can act as a reference for studying lake variations in alpine regions with limited observation data and provide a scientific basis for management policy under rapid climate change.

2. Materials and Methods

2.1. Study Area

The Yamzho Yumco Lake is the largest inland endorheic lake in the northern Himalayan Mountains, and it is located in Nagarze County. The broad definition of the lake basin includes the main lake and several surrounding lakes. Specifically, the Yamzho Yumco Lake has hydraulic connections with several surrounding lakes, including the Kongmu Co and Chen Co lakes, whereas it has no hydraulic connections with the neighboring Puma Yumco and Bajiu Co lakes [47]. Therefore, the present study considered the Yamzho Yumco Lake basin to include the basins of the Yamzho Yumco, Kongmu Co, and Chen Co lakes.

The Yamzho Yumco Lake basin extends between 90°08′–91°45′ E and 28°27′–29°12′ N and has an elevation of 4305–7195 m (Figure 1). The dominant land cover types in the basin include grassland, lake area, bare land, and glaciers, with areas of lakes and glacier of 676.6 km^2 and 57.6 km^2, respectively. As shown in Figure 2 and Table 1, although there has been an increasing trend in average annual precipitation of 17.4 mm/10a, the seasonal distribution of precipitation is uneven, with most (88.4%) occurring from June to September. The average temperature is 3.2 °C and the average temperature from November to March is below 0 °C, whereas that from April to October is above 0 °C. There has been an increasing trend in annual average air temperature of 0.34 °C/10a, with temperature showing obvious seasonal changes.

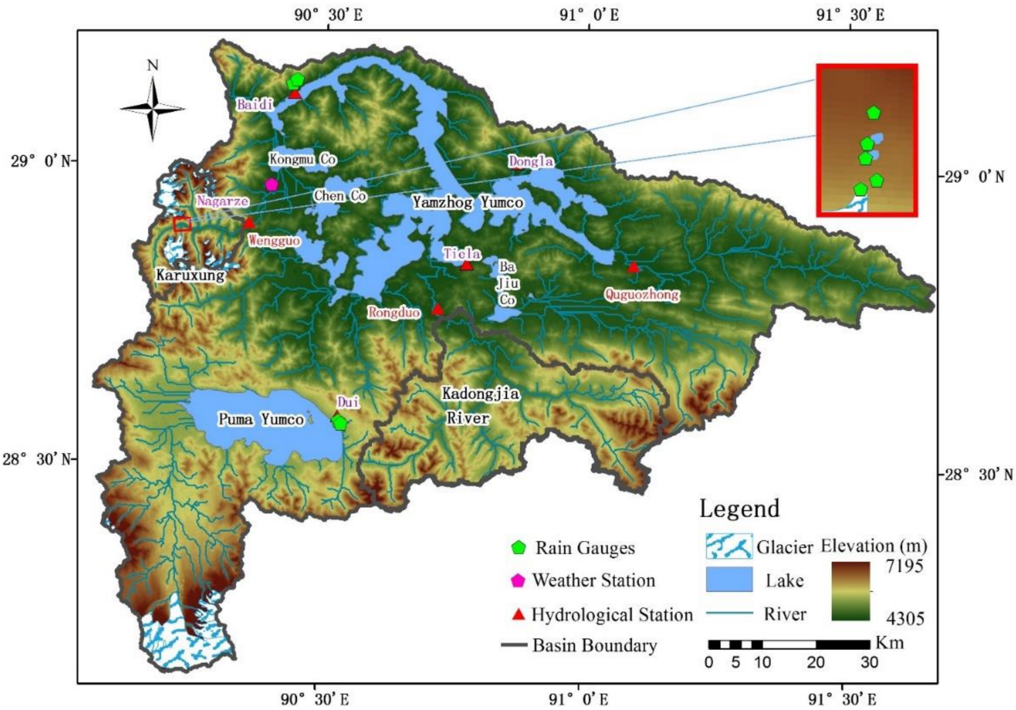

Figure 1. The Yamzho Yumco Lake Basin.

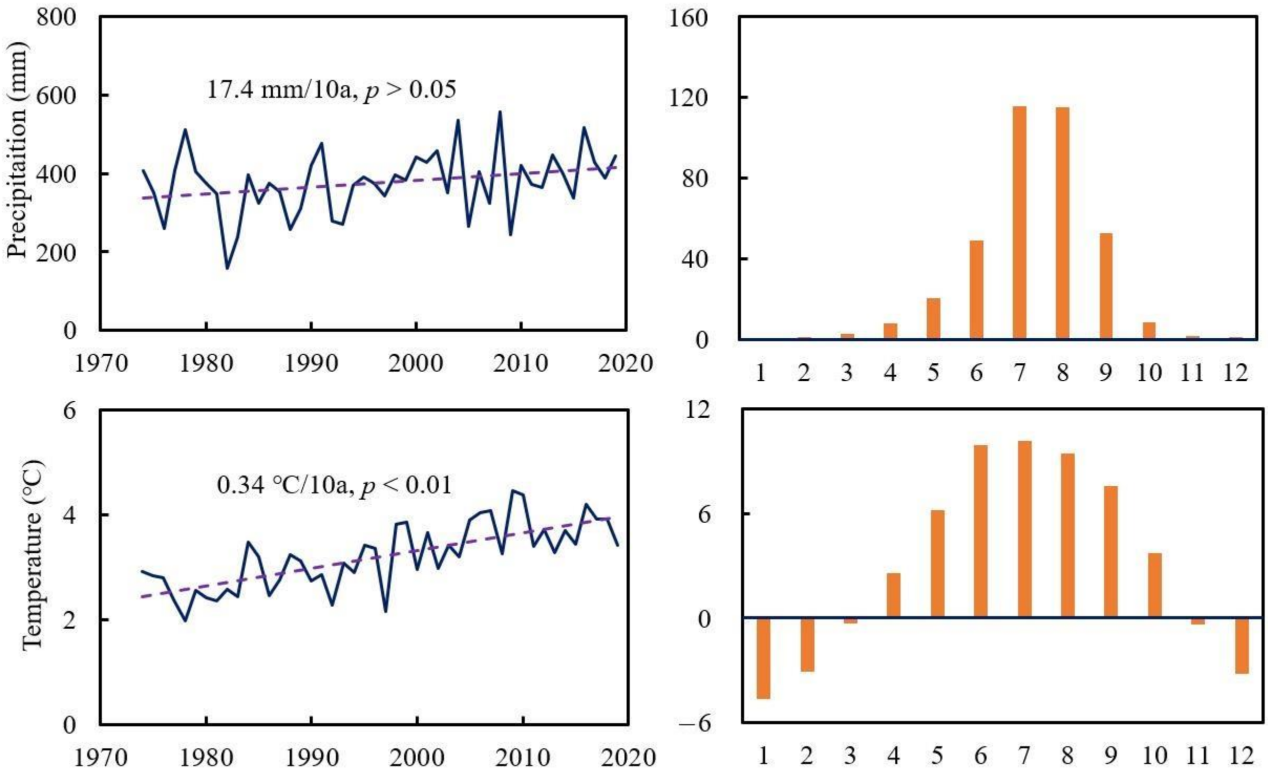

Figure 2. Interannual and seasonal variations of precipitation and temperature at the Nagarze station from 1974 to 2019.

Table 1. Statistics of meteorological data from 1974 to 2019 at the Nagarze weather station.

	Annual Temperature (°C)	Annual Precipitation (mm)
Minimum	2.0	159.1
Maximum	4.5	556.5
Average	3.2	376.3
Standard deviation	0.6	81.7

From east to west, sources of river runoff into the Yamzho Yumco, Kongmu Co, and Chen Co lakes include the non-glacial Gamalin, Kadongjia, Quqing, and Xiangda river catchments, and the glacial Puzong, Karuxong, and Yajian river catchments. Process contributing to runoff into the lakes include rainfall, snowmelt, and glacier melt. Quantitative estimations of surface runoff remain limited for the Yamzho Yumco Lake basin because of its high altitude and harsh weather conditions. Because long-term but discontinuous streamflow observations exist only for the Karuxung and Kadongjia rivers, during the model calibration and validation period, the two river catchments were selected to represent glacial and non-glacial regions, respectively, after which the model was extended to represent the entire basin.

2.2. Meteorological and Hydrologic Dataset

Meteorological data (1974–2019) were collected from the Nagarze meteorological station in the lake basin from the China Meteorological Science Data Service. The precipitation measurement could have systematic bias resulting from evaporation, wetting, and wind-induced losses, which could be corrected [48,49]. Daily discharge data within the Yamzho Yumco Lake basin was available from 1985 to 1994, 2006 to 2014 for the Karuxung river glacier catchment, and from 1983 to 1994 for the Kadongjia river non-glacial catchment. Although some rivers had runoff observations, the observation time was short and discontinuous; thus, a hydrological model could be used to simulate runoff to obtain long-term continuous runoff into the lake. During application to a study area, hydrological models were typically calibrated and validated against observed data to assess the accuracy of the model [50,51].

The available observations of precipitation at several gauging stations within the basin were not continuous, and most stations were not at a sufficiently high elevation to be representative of the study catchment. The present study identified the precipitation gradient in the study basin by installing five rain gauges in different locations with different altitudes of the basin from the August to September in 2013 and 2019.

Precipitation data input into a hydrological model have an important outcome on simulated runoff. However, only the Nagarze meteorological station provided long-term observations of precipitation that extended across the entire study period (Table 2). The present study obtained long-term precipitation data representative of the entire study area by combining precipitation data from Nagarze station, with the average precipitation gradient obtained from the HAR grid and eight surrounding grids.

Table 2. Description of the precipitation observation sites.

Item	Lat (°N)	Lon (°E)	Elevation (m)	Observation Period
Nagarze	28.967	90.4	4432	1974–2019
Dui	28.582	90.532	5109	1975–1978, 1984–2000, 2005–2012
Baidi	29.124	90.439	4467	1975–1994, 2001–2012
Wengguo	28.905	90.357	4577	1983–1995, 2005–2012
Rongduo	28.791	90.728	4566	1983–1995
Tiela	28.841	90.774	4458	1985–1990
Quguozhong	28.843	90.093	4426	1976–1978, 1985–1995
Dongla	29.011	90.869	4495	1983–1995
Rain gauge	28.877	90.229	5179	August–September in 2013
	28.876	90.227	5142	
	28.879	90.228	5071	
	28.88	90.224	5060	
	28.895	90.225	4832	
Rain gauge	29.128	90.445	4509	August–September in 2019
	29.129	90.447	4643	
	28.579	90.535	5029	
	28.578	90.534	5104	

2.3. Spatial and Remote Sensing Data

The spatial data included DEM data and data for land use, soil types, glacier extent, snow cover, and precipitation gradient. The DEM data were collected from the SRTM Digital Elevation Model with 90 m resolution (http://srtm.csi.cgiar.org/, accessed on 12 October 2022); land use data were obtained from GlobCover (http://due.esrin.esa.int/, accessed on 12 October 2022) [52] with 300 m resolution; glacier data were obtained from RGI data (http://glims.org/, accessed on 12 October 2022); soil type data were derived from the Harmonized World Soil Database (HWSD) (https://iiasa.ac.at/, accessed on 12 October 2022) [53]. Long-term timeseries data of SCA on the Tibetan Plateau (2003–2014) with 500 m resolutions were used for model parameter calibration. These data were derived by combining the Moderate Resolution Imaging Spectroradiometer (MODIS) v5 and Internet Map Server (IMS) datasets (https://data.tpdc.ac.cn/, accessed on 12 October 2022). The interpolation de-clouding algorithm was used to obtain a cloud-free product for the daily snow area [54]. The precipitation gradient was calculated based on the reanalyzed HAR v2 data (https://www.klima.tu-berlin.de/, accessed on 12 October 2022) [43] as it has been proved to more accurately reflect the altitude gradient of precipitation compared with other products and could provide more effective forcing data for hydrological models on the Tibetan Plateau [39,55,56]. In order to maximize hydrological model efficiency and accuracy, the data were resampled to a 300 m resolution to represent a higher precipitation spatial resolution in the study area.

2.4. J2000 Modeling

The J2000 hydrological model was applied to simulate inflow runoff and its different components based on limited observation data. This model was from Jena Adaptable Modelling System (JAMS) [57,58]. It was a process-based model, receiving spatial distribution attributes (including soil type, land use, et al.) from the HRU parameter file [59]. It consisted snow and glacier melt modules and has been successfully applied to several glacial basins including the Mapam Yumco, Paiku Co, Nam Co, and Tangra Yumco lake basins on the Tibetan Plateau [22], the Koshi River basin [60], and the Tamor basin [61]. In the structure of the J2000 hydrological model in Figure 3, snowmelt was affected by the temperature; the accumulated snow started to melt only when the temperature was above the threshold of the snow-melting temperature [62]. This model implemented a degree–day factor approach for glacier melt adapted from Hock [38] due to the limitation of plateau observation data. Components of simulated runoff were divided according to the model structure and the hydrological process generalization scheme [60]. Simulated runoff into the lake was divided into rainfall runoff, snowmelt runoff, glacier melt runoff, and baseflow considering the structural characteristics of the J2000 model and the approaches taken in previous studies using the Spatial Processes in Hydrology (SHPY) [10,63], SWAT model [64], and VIC model [37]. The present study considered baseflow to represent runoff produced by infiltration of rainfall and snowmelt into the deep groundwater layer. Therefore, the division of rainfall, snowmelt, and glacier components of runoff may not be completely consistent with those defined in other studies.

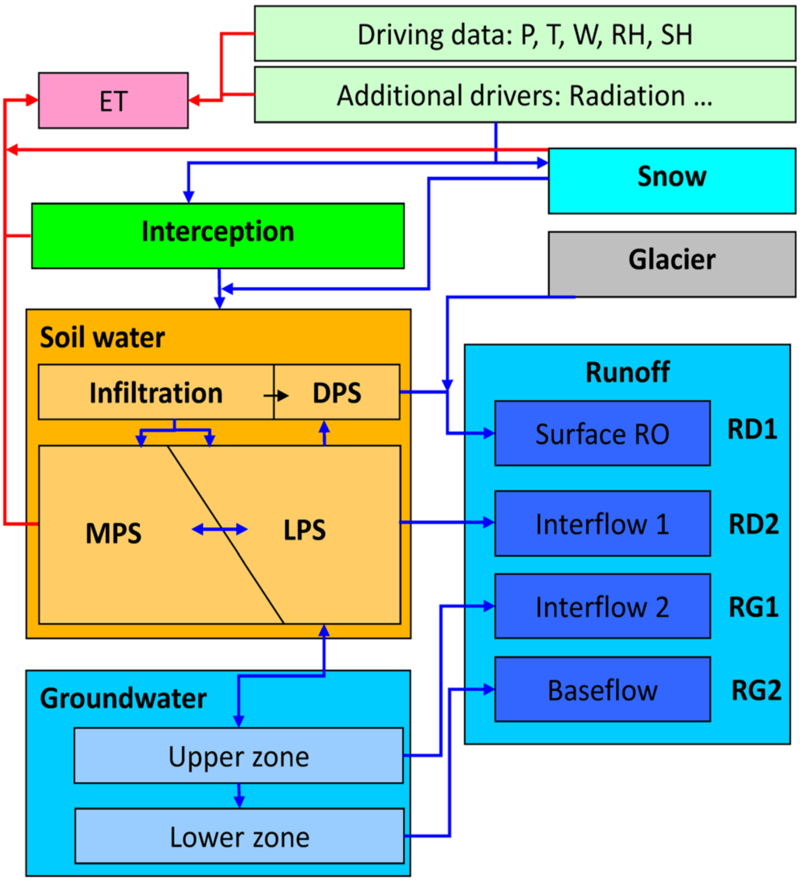

Figure 3. Structure of J2000 hydrological model (P: precipitation; T: temperature; W: wind speed; RH: relative humidity; SH: sunshine hour; LPS: large pore storage; MPS: middle pore storage; DPS: depression storage; RO: runoff) [62].

2.5. Evaluation Criteria

In order to validate model performance and forcing data, several goodness-of-fit statistical indexes, i.e., RMSE, NSE, R^2, and MARE were used [65]:

$$\text{RMSE} = \sqrt{\frac{1}{n}\sum_{i=1}^{n}(S_i - O_i)^2} \quad (1)$$

$$NSE = 1 - \frac{\sum_{i=1}^{n}(O_i - \overline{O})^2}{\sum_{i=1}^{n}(S_i - \overline{S})^2} \quad (2)$$

$$\text{R}^2 = \frac{\left[\sum_{\text{i}=1}^{\text{n}}(S_i - \overline{S})(O_i - \overline{O})\right]^2}{\sum_{\text{i}=1}^{\text{n}}(S_i - \overline{S})^2(O_i - \overline{O})^2}, \quad (3)$$

$$\text{MARE} = \frac{1}{N}\sum_{i=1}^{n}\left|\frac{S_i - O_i}{O_i}\right|, \quad (4)$$

where S_i is the simulated value, O_i is the observed value, $\overline{S}$ and $\overline{O}$ are the average value and observed value, respectively, and n is the number of observations.

This study obtained observations of daily runoff for 1983–1994 for the Kadongjia river catchment hydrological station. These runoff data in combination with the MODIS snow area data for 2003–2014 were used to calibrate and validate the hydrological model parameters in non-glaciated areas. The calibration and validation periods for runoff simulation were 1983–1990 and 1991–1994, respectively. The MODIS snow area data for 2003–2014 were used to validate the simulated snow area. Daily runoff data for 1985–1994 and 2006–2014 were obtained from the hydrological station of the Karuxung river catchment. The parameters of glacial area were obtained using the same method as for the non-glacial area. The calibration and validation periods for runoff simulation were 1985–1994 and 2006–2014, respectively. The parameters used with the model in the Karuxung and Kadongjia river catchments are shown in Table 3.

Table 3. Parameters used to simulate runoff in Karuxung and Kadongjia river catchments, Tibetan Plateau.

Parameters	Description (Units)	Values (Karuxung River)	Values (Kadongjia River)	Reasonable Range
BaseTemp	Snowmelt threshold temperature (°C)	0	0	−5–5
t_factr	Melt factor by sensible heat (mm/K)	1	3	0–5
r_factor	Melt factor by liquid precipitation (–)	0.1	3	0–5
g_factor	Melt factor by soil heat flow (mm)	0.1	3	0–5
meltFactorIce	Melt factor for ice melt (mm/K)	2	2	0–5
tbase	Threshold temperature for melt (°C)	−1	−1	−5–5
soilLinRed	Reduction coefficient for actual evapotranspiration (–)	0.95	3.45	0–10
soilMaxInfSummer	Maximum infiltration in summer (mm)	80	80	0–200
soilMaxInfWinter	Maximum infiltration in winter (mm)	90	90	0–200
soilLatVertLPS	Calibration coefficient for the distribution of interflow and percolation water (–)	1.2	1.2	0–10
soilConcRD1	Recession coefficient for overland flow (–)	6	6	0–10
soilConcRD2	Recession coefficient for interflow (–)	4.5	4.5	0–10
gwRG1RG2dist	RG1–RG2 distribution coefficient (–)	2	2	0–5
flowRouteTA	Run time of the outflow route (–)	20	20	0–100

2.6. Method

The detrending method can remove trends within timeseries data (such as temperature and precipitation) while retaining variation. This method can be used to analyze the impact of climatic factors on the total runoff and its component changes. The current study applied the Mann–Kendall (MK) test, which can be used to test the significance of the long-term change trend of the data series [65]. The linear trend analysis was used to fit the data by time series.

Precipitation gradients were calculated using the method as follows [48]:

$$P_i = P + (El_i - El) \times PG \quad (5)$$

where P_i is the corrected precipitation of the ith grid (mm), P is the precipitation of the Nagarze station (mm), El_i is the grid elevation (m), El is elevation of the Nagarze station (m), and PG is the calculated absolute precipitation gradient (mm/m).

Some studies have also used relative precipitation gradients [66]:

$$RPG = PG/P \times 100\% \quad (6)$$

where RPG is the relative precipitation gradient (%).

3. Results

3.1. Precipitation Correction

The spatial pattern of HAR precipitation data was assessed by comparing with rainfall observations from stations in the basin at different spatial scales. The blue color indicates higher precipitation, and the green color indicates lower precipitation; the HAR precipitation decreased from the surrounding mountain area to the central lake area (Figure 4). It exhibited higher precipitation data in the south, which is associated with higher elevation, and lower precipitation data in the west, which is associated with lower elevation. As shown in Figure 5, the seasonal distribution of the HAR data were consistent with that of observations from the Nagarze meteorological station. The HAR precipitation data showed high seasonality, with 86.1% of annual precipitation occurring from June to September, which was consistent with the rainfall observations from the Nagarze meteorological station (86.0%) between 2004 and 2018.

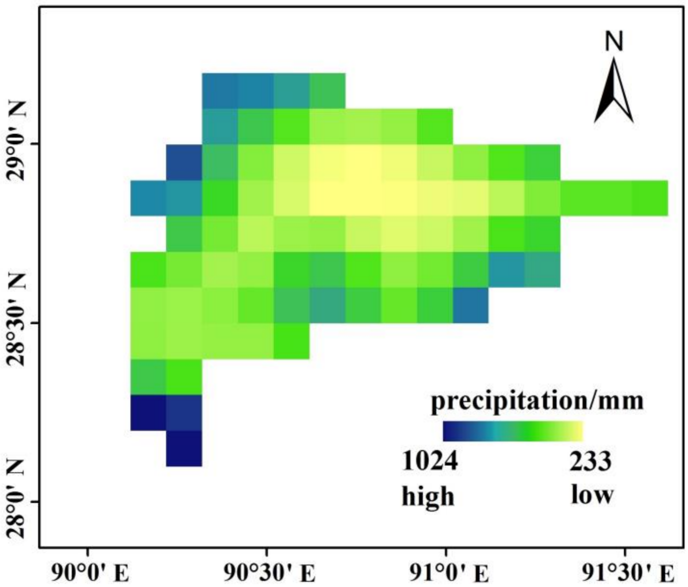

Figure 4. Spatial distribution of High Asia Refined (HAR) data in the Yamzho Yumco Lake basin, Tibetan Plateau.

However, long-term average annual HAR precipitation exceeded observed precipitation, indicating that although the HAR data overestimated annual precipitation in the study basin, it generally accurately represented the precipitation's spatial distribution. The accuracy of HAR precipitation's spatial distribution was evaluated based on the precipitation elevation gradient by comparing field observations in 2013 and 2019 in the north, west, and south of the basin with HAR data (Table 4).

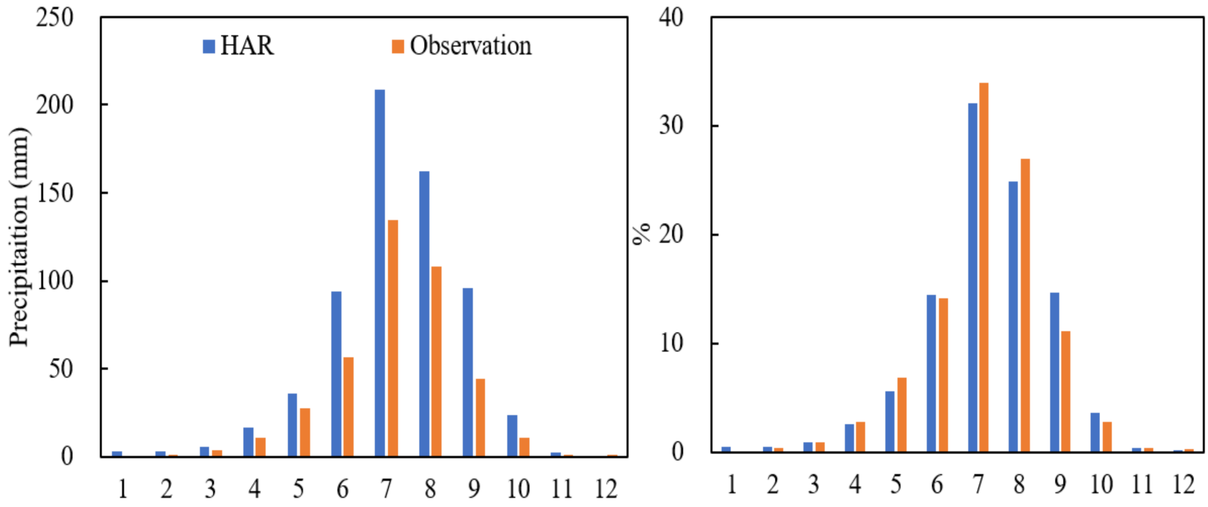

Figure 5. Comparison of annual average precipitation and seasonal distribution characteristics between HAR data and Nagarze weather station.

Table 4. Comparison of observed precipitation gradient and HAR precipitation gradient.

Location in the Basin	Time	Observed Precipitation Gradient (10^{-3} mm/m)	HAR Precipitation Gradient (10^{-3} mm/m)
North	August 2019	14.3	8.1
	September 2019	9.7	6.1
South	August 2019	−11.0	−6.0
	September 2019	−3.0	−2.0
West	August 2013	5.6	6.7
	September 2019	0.8	2.0

Because HAR data was not available in 2019, the monthly mean values of the 2004–2018 rain gauge grid points and the monthly mean values of the Nagarze station grid points were used to obtain the gradient of the multi-year monthly mean HAR precipitation gradient. As shown in Table 3, the gradients of observed and HAR precipitation were comparable. Therefore, the present study used precipitation data calculated by combining data from the Nagarze meteorological station with the HAR precipitation gradient in each grid as input data for runoff simulation. Thereafter, a precipitation dataset from 1974 to 2019 with 10 km spatial resolution was obtained, as shown in Figure 6, and the accuracy of the calculated precipitation data was evaluated by comparing its long-term average annual precipitation with that collected from several stations in the basin. The results showed that the calculated precipitation obtained by the precipitation gradient was closer to the observed rainfall in comparison to the original HAR precipitation, with a lower RMSE (56.0 mm/year vs. 147.7 mm/year). There was minimal difference between precipitation calculated using the absolute precipitation gradient and relative precipitation, although the precipitation calculated using the former was closer to observed rainfall. Therefore, the present study calculated precipitation using the absolute precipitation gradient.

3.2. Simulation of the Snow Cover Area

Simulation results of the SCA were compared with MODIS snow products to validate the model parameters' accuracies in both the glacial and non-glacial regions. Because cloud cover can affect the accuracy of the original MODIS snow data, a long-term timeseries of snow cover area was used for the TP for 2003 to 2014, as shown in Figure 7. The results showed good model performance within the simulation of snow cover, with R^2 values of 0.80 and 0.74 during 2003–2014 for the glacial and non-glacial regions, respectively. The simulated snow cover area showed a similar seasonal pattern to that of the observations, i.e., high values occurred in winter and spring, when temperatures were low, and low values occurred in summer, when temperatures were high. The R^2 values of SCA between simulation results and observations were 0.45 and 0.56 in glacial and non-glacial regions, respectively.

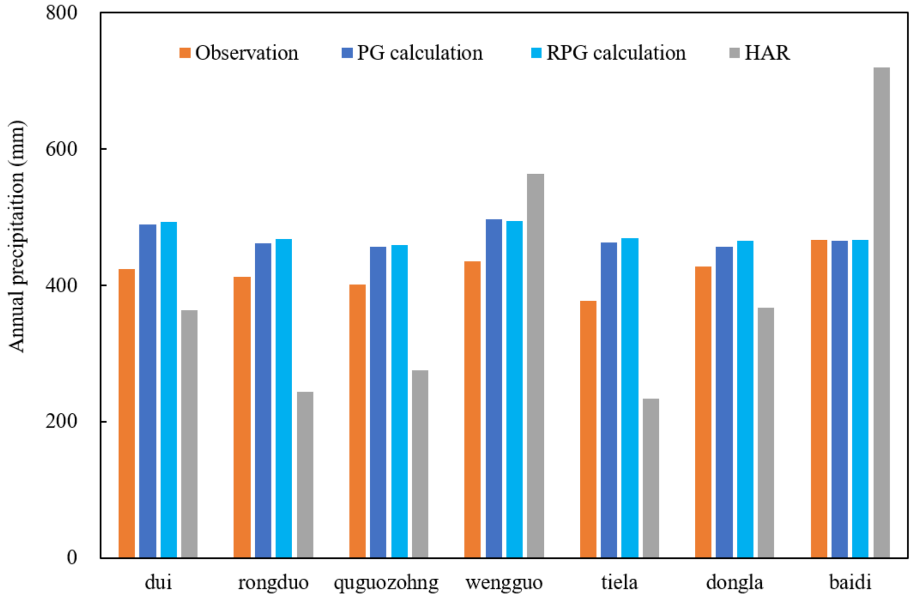

Figure 6. Comparison of the calculated precipitation, observed precipitation, and High Asia Refined (HAR) precipitation in the Yamzho Yumco Lake basin, Tibetan Plateau.

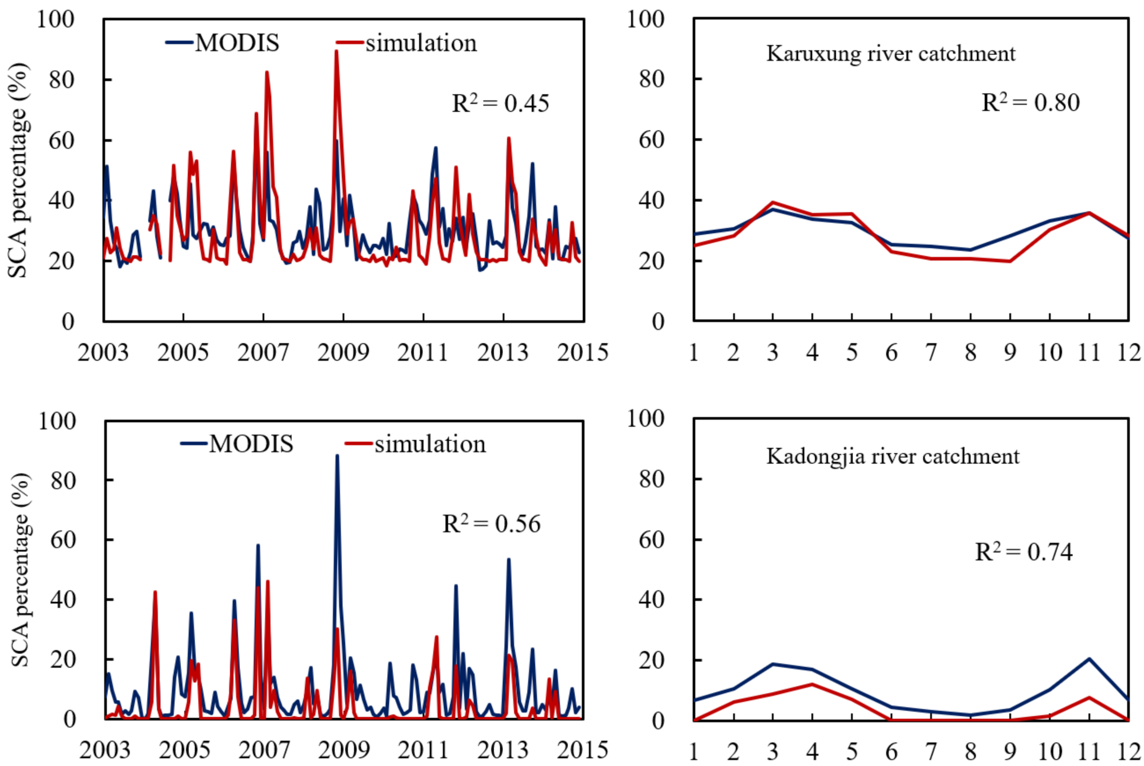

Figure 7. Monthly SCA simulation compared with MODIS data during 2003–2014.

3.3. Runoff Simulation

Sunshine duration, relative humidity, wind speed, and the maximum, minimum, and mean temperatures observed at the Nagarze meteorological station were selected as forcing data for the J2000 model's runoff simulation. The hydraulic parameters were calibrated using the observed discharge data at the Karuxung and Kadongjia river catchments to represent the parameters in glacial and non-glacial regions. As shown in Figure 8, the simulated runoff was compared to observations at the Karuxung and Kadongjia river catchments at different periods.

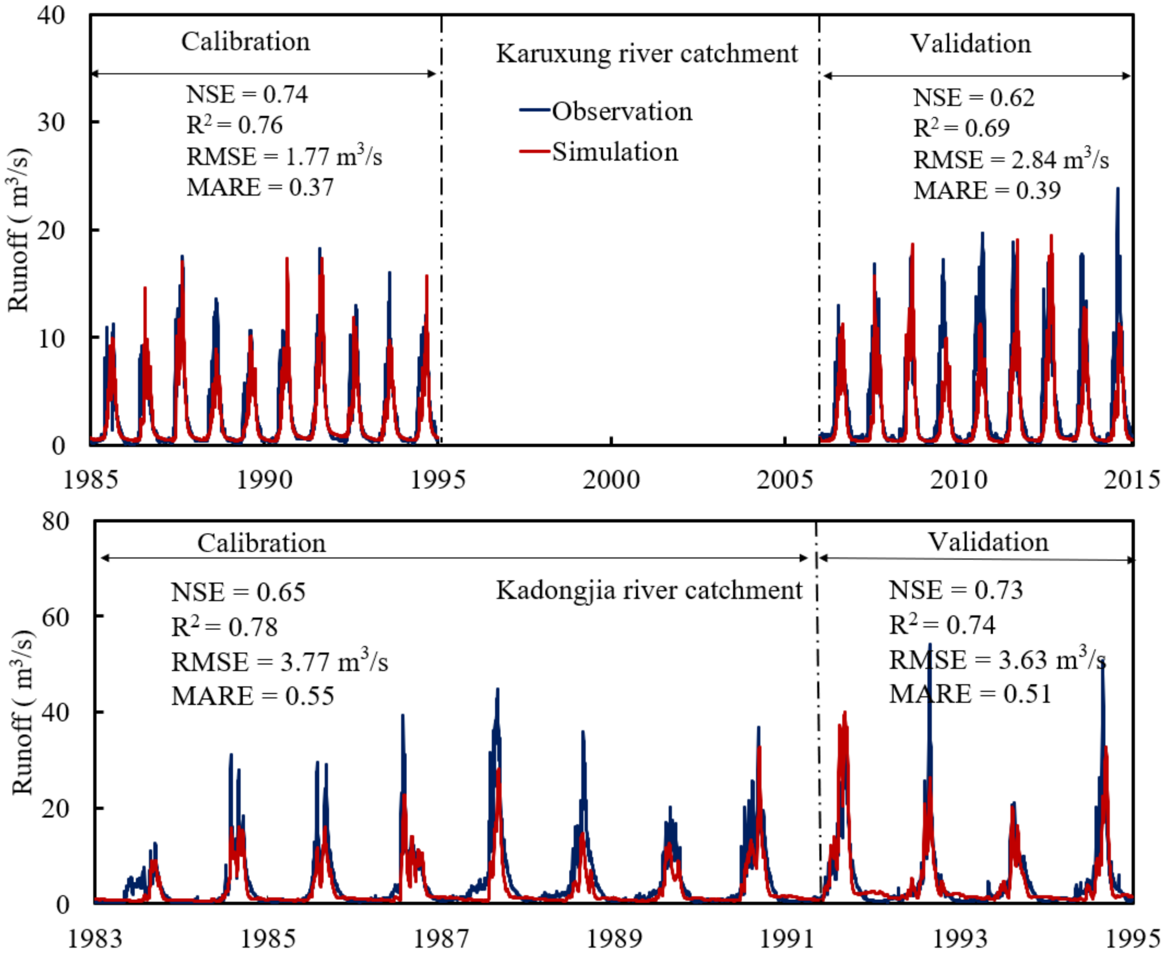

Figure 8. Daily observed and simulated discharges in the glacial region and non-glacial region.

The model obtained acceptable runoff simulations for the Karuxung river catchment, with NSE, R^2, MARE and RMSE values of 0.74, 0.76, 0.37, and 1.77 m^3/s for the calibration period, respectively, and 0.62, 0.69, 0.39, and 2.84 m^3/s for the validation period, respectively. As shown in Figure 9, snowmelt runoff contributed 3.8%, 3.1%, and 3.4%, glacier melt runoff contributed 58.0%, 60.8%, and 59.2%, rainfall runoff contributed 32.6%, 29.5%, and 31.5%, and baseflow contributed 5.6%, 6.7%, and 5.9% of the total runoff during calibration, validation, and the entire study period, respectively. Moreover, the model also achieved acceptable performance of runoff simulation for the Kadongjia river catchment, with NSE, R^2, MARE, and RMSE values of 0.65, 0.78, 0.55, and 3.37 m^3/s during the calibration period and 0.73, 0.74, 0.51 and 3.63 m^3/s during the calibration period, respectively. As shown in Figure 9, snowmelt runoff contributed 1.5%, 0.5%, and 1.2%, rainfall runoff contributed 59.8%, 61.9%, and 60.5%, and baseflow contributed 38.7%, 37.6%, and 38.3% of the total runoff during the calibration period, validation period, and the entire study period, respectively.

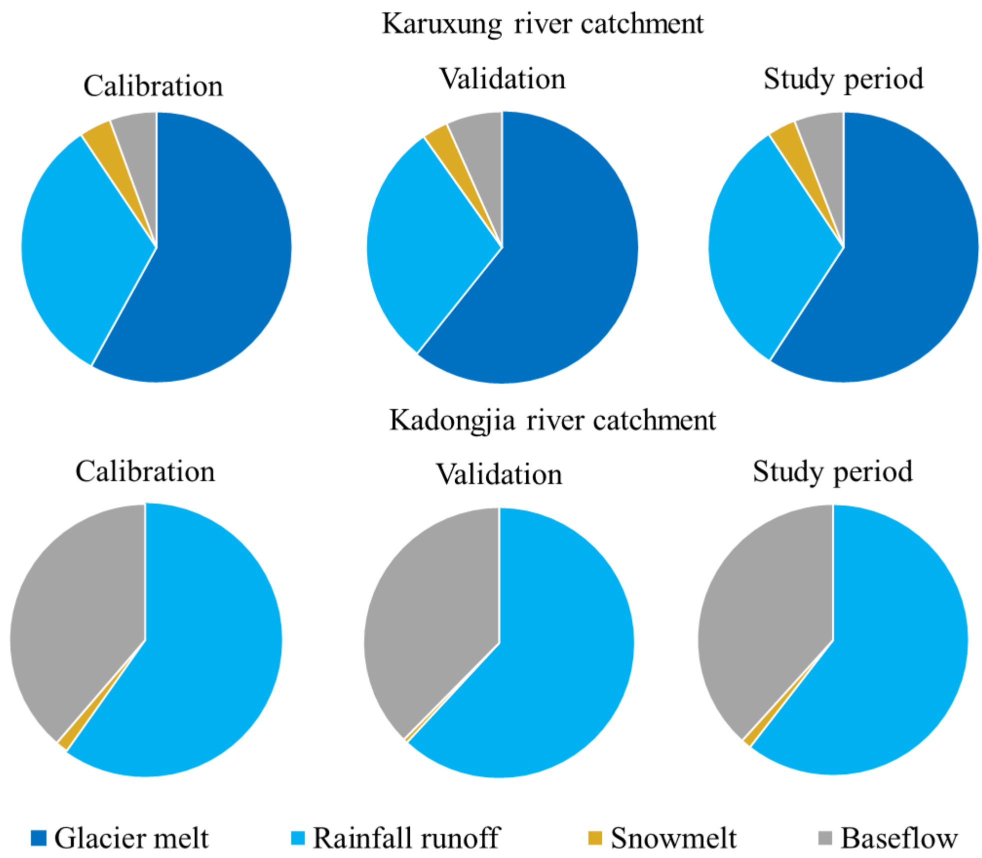

Figure 9. Different components of runoff and their contributions.

3.4. Long-Term and Seasonal Changes to Lake Inflow

Simulated results of long-term runoff for both the glacial and non-glacial regions during 1974 to 2019 are as shown in Figure 10. The results showed that the total runoff in the Karuxung river catchment increased significantly ($p < 0.05$) at the rate of 9.2 mm/10a. There was a fluctuating but insignificant decreasing trend in snowmelt runoff −0.1 mm/10a ($p > 0.05$). There were insignificant increases in both glacier melt and rainfall runoff ($p > 0.05$) at the rate of 4.5 mm/10a and 4.4 mm/10a, respectively. There were insignificant increases in both total runoff and rainfall runoff in the Kadongjia river catchment ($p > 0.05$) with growth rates of 5.7 mm/10a and 4.1 mm/10a, respectively. There was a downward fluctuating but insignificant trend in snowmelt runoff of −0.2 mm/10a ($p > 0.05$).

The monsoon (May to September) was the main factor driving seasonal changes in runoff in both the Karuxung and Kadongjia river catchments. Summer rainfall runoff and glacier melt both showed high contributions to annual total runoff in the Karuxung river catchment due to the high precipitation and temperature of this basin, whereas snowmelt runoff showed two peaks corresponding with spring and autumn, which was consistent with the seasonal changes in SCA. Summer and autumn rainfall runoff showed high contributions to annual runoff in the Kadongjia river catchment due to this period corresponding with higher rainfall.

Figure 11 shows the results of the long-term modeling of runoff for the entire lake basin. The average runoff into the lake was $5.5 \pm 1.4 \times 10^8$ m^3/10a from 1974 to 2019, with rainfall runoff, snowmelt runoff, glacier melt runoff, and baseflow contributed 3.0×10^8 m^3/10a (54.6%), 0.1×10^8 m^3/10a (1.8%), 0.6×10^8 m^3/10a (10.9%), and 1.8×10^8 m^3/10a (32.7%) of the total runoff, respectively. Seasonal changes in glacier melt were mainly driven by air temperature, with the peak occurring in summer. Snowmelt runoff mainly occurred in spring and autumn. Runoff in spring, summer, autumn, and winter contributed to 8.6%, 57.4%, 24.9%, and 9.1% of annual total runoff, respectively, because the rainfall was affected by the monsoon.

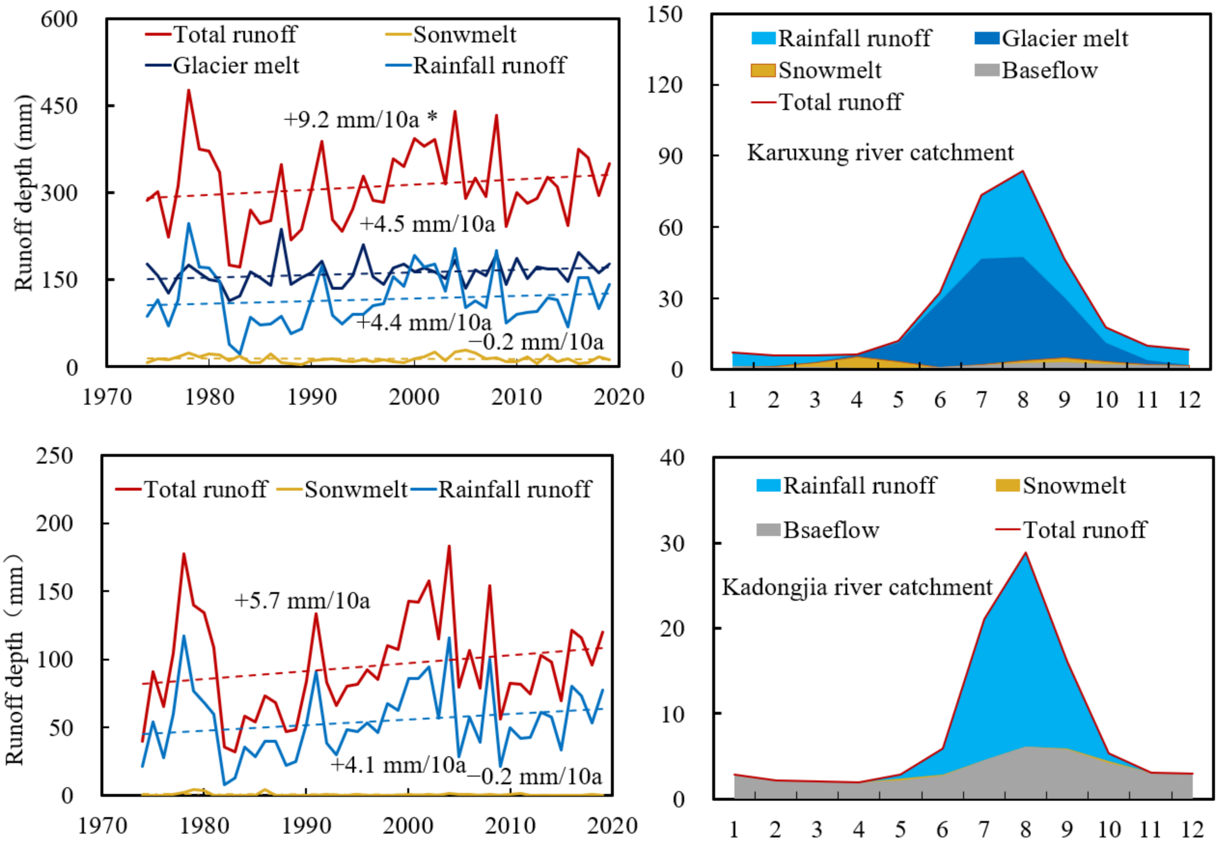

Figure 10. The changing trends of the total runoff and its components in the glacial region and non-glacial region from 1974 to 2019 (*: $p < 0.05$).

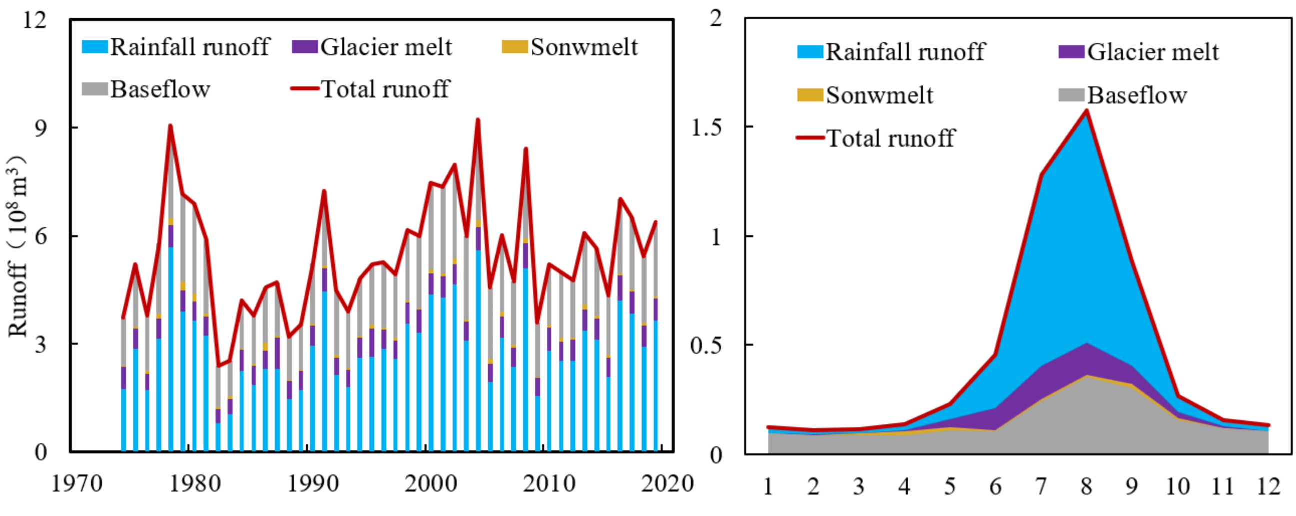

Figure 11. Annual and intra-annual variations of runoff and its components of Yamzho Yumco lake basin.

Among these components, the contribution of snowmelt runoff, glacier melt runoff, and baseflow to total runoff decreased, whereas the rainfall runoff contribution increased at a rate of 1.0%/10a from 1974 to 2019. Although the melt runoff increased, the proportion of melt runoff decreased at the rate of 0.07%/10a, indicating the change in rainfall runoff was the main factor in the variation of total runoff.

The contributions of glacial and non-glacial regions to total runoff in the study period were 31.4% and 68.6%, respectively, whereas these two areas accounted for 19.2% and 80.8%

of the total area, respectively. This result indicates that there were increased inflows from glacier melt and snowmelt into the lake in glacial regions, thereby confirming that climate change affects different regions differently.

4. Discussion

4.1. Uncertainties in Runoff Simulation

Precipitation could affect lake change via surface runoff. This study used the combination of meteorological station observation data and HAR distribution data to obtain more accurate precipitation data for the study basin in terms of both quantity and spatial distribution. The main difficulty of precipitation distribution in Tibetan Plateau lied in the large spatial-temporal difference of precipitation and the scarcity of observation sites. On one hand, the spatial variability of precipitation increased with the increase of the topographic effect [67,68]. On the other hand, the study area had only one long-term meteorological observation station and was located next to the lake at a lower altitude, whereas hillside and peak stations were scarce. Therefore, due to the spatial variability of precipitation, it was possible that when it was raining in certain places in the basin, the observation station did not observe it, which would cause errors. The low values of the metrics are probably due to the large spatial variability of precipitation in the study basin; thus, we corrected precipitation by using the combination of HAR and field observation precipitation data for the study basin. The NSE values of the daily runoff simulation in glacial and non-glacial river catchment were 0.74 and 0.65 during the calibration period, respectively. Although the index of NSE meets the requirement of more than 0.5 [69], both the glacial and non-glacial river catchments have some distance with the weather station; thus, there was some uncertainty about precipitation, which would affect the daily runoff simulation.

There was a peak in SCA in November corresponding with the drop in temperature and increase in snowfall. There was an increase in SCA corresponding with the later decrease in precipitation events and increase in snow sublimation. The increased precipitation and lower temperature in early spring resulted in another SCA peak. With the continuing rise in temperature, snow continued to melt, reaching a minimum coverage in summer. The changing patterns observed in the present study showed good consistency with those observed in previous results [70]. Accurate SCA data is an essential precondition for improved simulation of runoff. The lowest temperature recorded in summer reached 4.8 °C, which should correspond with a low SCA. Therefore, the presence of low SCA values during summer in the MODIS snow products may be due to cloud interference [71]. Aside from snow melt, runoff from glacier melt was identified as an additional source of runoff inflow in the Yamzho Yumco Lake. Therefore, there was a need to calculate glacier melt runoff contribution. The calculation of total runoff into the lake in the glacial region was dependent on the degree-of-day factor, with the difference in the values of this factor for bare ice and moraine-covered glaciers ignored. The present study did not consider spatial and temporal variations in daily ice and snow factors at different elevations, thereby introducing uncertainty into the simulations of the glacier melt path.

4.2. Comparison with Other Alpine Lake Studies

Corrected precipitation data was employed as the forcing data to drive the J2000 model for runoff simulation in our study. Results showed that snowmelt runoff of the Kadongjia river catchment for the non-glaciated area of the Yamzho Yumco Lake basin accounted for about 1.2% of the total streamflow. This was consistent with Sun et al. [47], who found that snowmelt runoff accounted for about 4.0% of the annual runoff in the Kadongjia river catchment during 1974 to 2010 by using the SWAT model. Moreover, rainfall runoff, glacier melt runoff, and snowmelt runoff accounted for 31.5%, 59.2%, and 3.4%, respectively, of the total stream-flow in the Karuxung river catchment for the glaciated area of the Yamzho Yumco Lake basin. These results were comparable with Zhang et al. [18], who reported that rainfall runoff, glacier melt runoff, and snowmelt runoff accounted for 34.1%, 61.9%, and 4.0%, respectively, of the total streamflow for the Karuxung river catchment based on observed precipitation data from the Nagarze meteorological station and SRM (Snowmelt Runoff) model. Compared with the corrected precipitation, simulations of rainfall runoff, glacier melt runoff, snowmelt runoff, and baseflow driven by the original observation data accounted for 23.6%, 67.4%, 3.8% and 5.2%, respectively, of the total streamflow for the Karuxung river catchment, indicating that inaccurate precipitation data might induce lower rainfall runoff and higher glacier melt and snowmelt runoff to maintain water balance in the model [72]. Therefore, the combination of HAR and filed observation could reduce the uncertainty of model-induced precipitation inputs.

The changes in alpine lakes were mainly affected by variations of precipitation, evaporation, and runoff within the lake basins. Therefore, lakes showed different changing trends in different regions over the Plateau as induced by various principal impact factors under different climate backgrounds, i.e., most lakes in the central and northern TP expanded rapidly, whereas some lakes in the south shrunk since the 1990s [73]. For the impact factors, Nam Co and Selin Co were often studied as examples of expanding lakes through various hydrological models such as WEB-DHM, VIC, J2000, etc. All results showed that the increases in rainfall runoff and glacier melt runoff were the main factors for the expansion of the two lakes [22,23,26]. For the shrinking lakes, e.g., Paiku Co in the southern TP, excessive evaporation was considered the primary influencing factor for the shrinkage, but the increase in runoff into the lake reduced the lake'schange [22]. For the fastest declining lake on the Tibetan Plateau, Li et al. [31] found that the main reason for the change in Yamzho Yumco Lake was the combination of a decrease in precipitation and an increase in temperature, which led to more water consumption through evaporation than recharge by glacier melt runoff under a warming climate from 2004 to 2014 by using the runoff coefficient method. Based on the simulation results of the J2000 model, we found the decrease in rainfall runoff could also lead to the decrease in total runoff to the lake in addition to the influences of changing glacier melt runoff and evaporation.

Beyond the TP, water levels of alpine lakes in the Brazilian Plateau, South African Plateau and Central Siberian Plateaus have reported rising trends mainly driven by increasing precipitation and surface runoff [74]. Two adjacent lakes in central Asia showed changes as well. Lake Karakul showed rising water levels mainly due to increased glacier melt runoff, whereas the other lake, Lake Chatyrkul, showed a decline caused by increased evaporation under the same warming background [75]. Except for the natural factors, human activity is usually another important impact factor that can influence the changes of alpine lakes. For example, human activity contributed to more than half of the total decline in lake levels for Lake Victoria in the East African Plateau during 2004–2005 [76], and it was also the primary influencing factor for the rapid shrinkage of the Aral Sea in Central Asia [77]. Previous studies have pointed out that the Yamzho Yumco Lake's water level had continued to rise from 1974 to 2005 due to increases in precipitation and surface runoff, then declined from 2005 to 2016 due to the newly constructed hydropower station, and then returned to rising again after the hydropower station shut down after 2017 [36,37,78].

4.3. Impact of Climate Change on Runoff

The Tibetan Plateau underwent significant warming over recent decades, with warming magnitude gradually increasing from south to north [79,80]. Similarly, the precipitation variation of the Tibetan Plateau also showed significant spatial differences, i.e., precipitation decreased in the south but increased in the east and northwest [81,82]. However, this present study found that both temperature and precipitation were increased in Yamzho Yumco Lake, which is located in the southern Tibetan Plateau, a finding confirmed by previous local scale studies [83,84]. This differently changing pattern might be caused by the influence of the complex topography. A detrended analysis method was applied to identify temperature and precipitation impacts on runoff and its components without considering the impacts of their long-term trends.

Figure 12 shows the timeseries of temperature and precipitation, which illustrated interannual changes in the glacial and non-glacial regions, i.e., the Karuxung river catchment and the Kadongjia river catchment. The total runoff, snowmelt, glacier melt, and rainfall runoff in the Karuxung river catchment decreased by 8.6%, 3.4%, 12.1%, and 3.2%, respectively, after removing the effect of the trend in precipitation. Under stable precipitation, the increase in temperature resulted in an increase of meltwater, which offset the increase in evaporation. Therefore, after removing the long-term trend in temperature, total runoff and glacier melt runoff decreased by 6.0% and 14.5%, respectively, whereas snowmelt runoff and rainfall runoff increased by 4.7% and 7.9%. A comparison of simulated runoff with or without the consideration of precipitation and temperature trends showed that precipitation had a greater impact on runoff than temperature, indicating that runoff was more sensitive to precipitation in glacial regions.

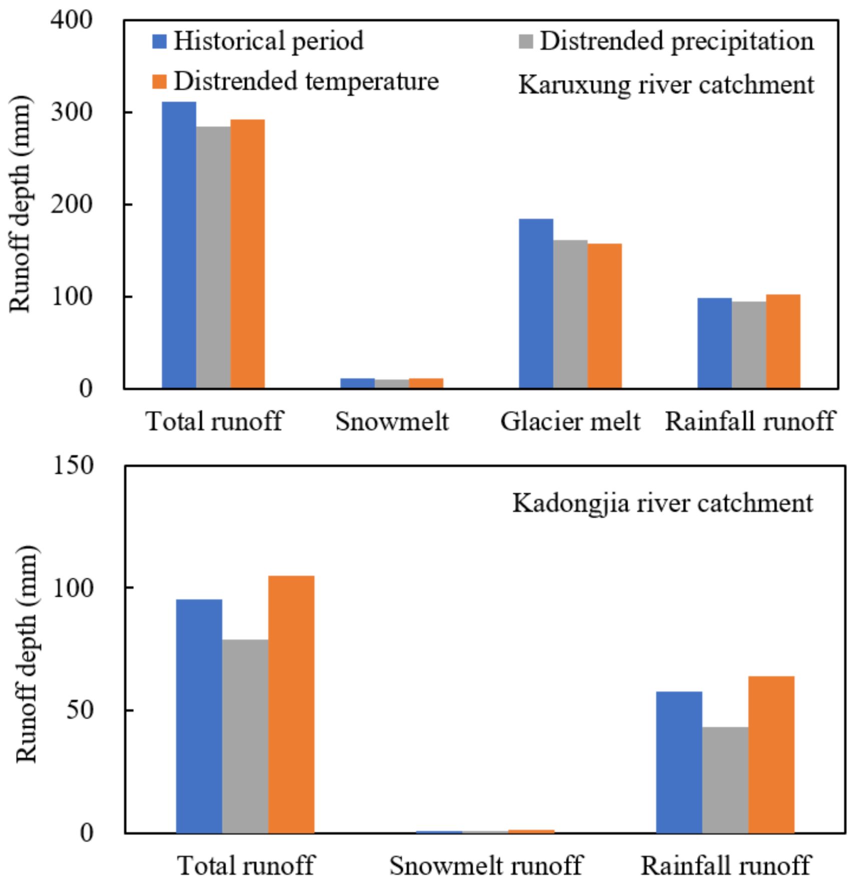

Figure 12. The response of total runoff and its component to climate variables for glacial and non-glacial regions.

Total runoff, snowmelt, and rainfall runoff in the Kadongjia river catchment decreased by 16.9%, 24.8%, and 25.1%, respectively, after removing the long-term trend in precipitation, whereas they increased by 10.4%, 31.2%, and 11.3%, respectively, when removing the long-term trend in temperature. The relative change in snowmelt with increasing temperatures exceeds that of other runoff forms because of the smaller snowmelt runoff. Lower temperatures can result in increased snow, which increases snowmelt runoff. Due to the decrease in temperature, the evaporation effect was weakened, which led to the increase of rainfall runoff. The increase in total runoff could be attributed to increases in precipitation and temperature, with runoff more sensitive to precipitation in non-glacial regions.

In the glacial and non-glacial regions, the effect of precipitation on runoff behaves consistently: under the same temperature conditions, although the magnitude of change was different, increasing precipitation increased runoff, and decreasing precipitation decreased runoff. However, there were differences between the temperature response of the runoff in the glacial and non-glacial regions. Under the same precipitation conditions in the glacial regions, higher temperatures increased melt runoff and total runoff; this was also supported by studies in some glacier-dominated watersheds [85].

In the non-glacial regions, higher temperatures increased evaporation and decreased total runoff, and this had a negative effect on the runoff; this was also supported by studies in some watersheds with low percentages of glaciers [86,87]. Although the differences between glacial and non-glacial runoff responses to climate change exist, surface runoff into the lake was more sensitive to precipitation than to temperature in both glacial and non-glacial regions.

5. Conclusions

The major findings include: (1) the precipitation obtained by the observation station combined with reanalysis data could effectively reflect the spatial distribution of precipitation in alpine lake basins and reduce the error of reanalysis data of 61.2%; (2) the average annual runoff into the Yamzho Yumco Lake from 1974 to 2019 was $5.5 \pm 1.4 \times 10^8$ m^3/10a, with rainfall runoff, snowmelt, glacier melt, and baseflow contributing 54.6%, 1.8%, 10.9%, and 32.7% to the annual total runoff, respectively; (3) runoff in summer, autumn, winter, and spring accounted for 60.6%, 23.9%, 8.8%, and 6.7% of the annual runoff, respectively; (4) surface runoff into the lake was more sensitive to precipitation than temperature in both glacial and non-glacial regions. In glacial areas, the reduction in total runoff after removing the precipitation trend was 1.4 times than that of temperature, and in non-glacial areas, the reduction in total runoff after removing the precipitation trend was 1.6 times than the increase in total runoff after removing the temperature trend.

Under the background of climate change, the rainfall runoff proportion to total runoff increased at a rate of 1.0%/10a, whereas the melt runoff proportion decreased at a rate of 0.07%/10a, indicating the change in rainfall runoff was the main factor of the variation of total runoff. As the basin becomes warmer and wetter, the lake level could be restored in the future, excluding anthropogenic interference, under the current climate changing pattern.

Usually, accurate precipitation is difficult to obtain in remote alpine basins such as the Tibetan Plateau. This study may provide a reference to hydrological study in these data-scarce remote areas with an improved, more accurate precipitation dataset obtained through combining a high-resolution reanalysis product and a short-term field observation. In this research, on-site observations of precipitation and runoff greatly assisted in increasing the accuracy of simulations of runoff and its components to further improve the understanding of hydrological processes in data-scarce areas. More accurate precipitation and different runoff components have been obtained in the Yamzho Yumco Lake basin; this will help us further quantitatively reveal the changing mechanisms of an alpine lake which has been the fastest-declining lake on the southern Tibetan Plateau and to know the key factor that affected the lake's water volume through the water balance method over the past four decades. This future research will also provide a policy basis for local water resource management, ecological sustainability, and quantitative analysis.

Author Contributions: Conceptualization, F.Z.; data curation, H.T. and Y.X.; funding acquisition, F.Z.; methodology, L.W.; project administration, C.Z.; software, H.Z.; visualization, H.T.; writing—original draft, H.T., F.Z. and C.Z.; writing—review and editing, H.T. and Z.Y. All authors have read and agreed to the published version of the manuscript.

Funding: This research was funded by [National Natural Science Foundation of China] grant number [41771090] and grant number [41988101-03].

Data Availability Statement: Not applicable.

Conflicts of Interest: The authors declare that they have no known competing financial interest or personal relationship that could have appeared to influence the work reported in this paper.

References

1. Immerzeel, W.W.; Pellicciotti, F.; Bierkens, M.F. Rising river flows throughout the twenty-first century in two Himalayan glacierized watersheds. *Nat. Geosci.* **2013**, *6*, 742–745. [CrossRef]
2. Immerzeel, W.W.; Lutz, A.F.; Andrade, M.; Bahl, A.; Biemans, H.; Bolch, T.; Baillie, J. Importance and vulnerability of the world's water towers. *Nature* **2020**, *577*, 364–369. [CrossRef] [PubMed]
3. Liu, Z.; Yao, Z.; Wang, R.; Yu, G. Estimation of the Qinghai-Tibetan Plateau runoff and its contribution to large Asian rivers. *Sci. Total Environ.* **2020**, *749*, 141570. [CrossRef]
4. Shukla, S.; Jain, S.; Kansal, M. Hydrological modelling of a snow/glacier-fed western Himalayan basin to simulate the current and future streamflows under changing climate scenarios. *Sci. Total Environ.* **2021**, *795*, 148871. [CrossRef] [PubMed]
5. Gao, H.; Feng, Z.; Zhang, T.; Wang, Y.; He, X.; Li, H.; Duan, Z. Assessing glacier retreat and its impact on water resources in a headwater of Yangtze River based on CMIP6 projections. *Sci. Total Environ.* **2021**, *765*, 142774. [CrossRef] [PubMed]
6. Kraaijenbrink, P.D.; Bierkens MF, P.; Lutz, A.F.; Immerzeel, W.W. Impact of a global temperature rise of 1.5 degrees Celsius on Asia's glaciers. *Nature* **2017**, *549*, 257–260. [CrossRef] [PubMed]
7. Lv, A.; Qi, S.; Wang, G. Multi-model driven by diverse precipitation datasets increases confidence in identifying dominant factors for runoff change in a subbasin of the Qaidam Basin of China. *Sci. Total Environ.* **2021**, *802*, 149831. [CrossRef] [PubMed]
8. Yang, W.; Jin, F.; Si, Y.; Li, Z. Runoff change controlled by combined effects of multiple environmental factors in a headwater catchment with cold and arid climate in northwest China. *Sci. Total Environ.* **2021**, *756*, 143995. [CrossRef]
9. Lutz, A.F.; Immerzeel, W.W.; Shrestha, A.B.; Bierkens MF, P. Consistent increase in High Asia's runoff due to increasing glacier melt and precipitation. *Nat. Clim. Change* **2014**, *4*, 587–592. [CrossRef]
10. Kong, Y.; Pang, Z. Evaluating the sensitivity of glacier rivers to climate change based on hydrograph separation of discharge. *J. Hydrol.* **2012**, *434*, 121–129. [CrossRef]
11. Goodarzi, M.R.; Sabaghzadeh, M.; Mokhtari, M.H. Impacts of aspect on snow characteristics using remote sensing from 2000 to 2020 in Ajichai-Iran. *Cold Reg. Sci. Technol.* **2022**, *204*, 103682. [CrossRef]
12. Li, Z.; Lyu, S.; Chen, H.; Ao, Y.; Zhao, L.; Wang, S.; Meng, X. Changes in climate and snow cover and their synergistic influence on spring runoff in the source region of the Yellow River. *Sci. Total Environ.* **2021**, *799*, 149503. [CrossRef] [PubMed]
13. Shen, Y.; Shen, Y.; Fink, M.; Kralisch, S.; Chen, Y.; Brenning, A. Trends and variability in streamflow and snowmelt runoff timing in the southern Tianshan Mountains. *J. Hydrol.* **2017**, *557*, 173–181. [CrossRef]
14. Song, C.; Huang, B.; Ke, L.; Richards, K.S. Seasonal and abrupt changes in the water level of closed lakes on the Tibetan Plateau and implications for climate impacts. *J. Hydrol.* **2014**, *514*, 131–144. [CrossRef]
15. Zhang, G.; Luo, W.; Chen, W.; Zheng, G. A robust but variable lake expansion on the Tibetan Plateau. *Sci. Bull.* **2019**, *64*, 1306–1309. [CrossRef]
16. Zhang, G.; Yao, T.; Chen, W.; Zheng, G.; Shum, C.K.; Yang, K.; Piao, S.; Sheng, Y.; Yi, S.; Li, J.; et al. Regional differences of lake evolution across China during 1960s–2015 and its natural and anthropogenic causes. *Remote Sens. Environ.* **2019**, *221*, 386–404. [CrossRef]
17. Qiao, B.; Zhu, L. Difference and cause analysis of water storage changes for glacier-fed and non-glacier-fed lakes on the Tibetan Plateau. *Sci. Total Environ.* **2019**, *693*, 133399. [CrossRef]
18. Zhang, F.; Zhang, H.; Hagen, S.C.; Ye, M.; Wang, D.; Gui, D.; Zeng, C.; Tian, L.; Liu, J. Snow cover and runoff modelling in a high mountain catchment with scarce data: Effects of temperature and precipitation parameters. *Hydrol. Process.* **2015**, *29*, 52–65. [CrossRef]
19. Li, B.; Zhang, J.; Yu, Z.; Liang, Z.; Chen, L.; Acharya, K. Climate change driven water budget dynamics of a Tibetan inland lake. *Glob. Planet. Change* **2017**, *150*, 70–80. [CrossRef]
20. Zhang, G.; Yao, T.; Shum, C.K.; Yi, S.; Yang, K.; Xie, H.; Feng, W.; Tobias, B.; Wang, L.; Ali, B.; et al. Lake volume and groundwater storage variations in Tibetan Plateau's endorheic basin. *Geophys. Res. Lett.* **2017**, *44*, 5550–5560. [CrossRef]
21. Qiao, B.; Zhu, L.; Yang, R. Temporal-spatial differences in lake water storage changes and their links to climate change throughout the Tibetan Plateau. *Remote Sens. Environ.* **2018**, *222*, 232–243. [CrossRef]
22. Biskop, S.; Maussion, F.; Krause, P.; Fink, M. Differences in the water-balance components of four lakes in the southern-central Tibetan Plateau. *Hydrol. Earth Syst. Sci.* **2016**, *20*, 209–225. [CrossRef]
23. Zhong, X.; Wang, L.; Zhou, J.; Li, X.; Qi, J.; Song, L.; Wang, Y. Precipitation dominates long-term water storage changes in Nam Co Lake (Tibetan Plateau) accompanied by intensified cryosphere melts revealed by a basin-wide hydrological modelling. *Remote Sens.* **2020**, *12*, 1926. [CrossRef]
24. Zhu, L.; Xie, M.; Wu, Y. Quantitative analysis of lake area variations and the influence factors from 1971 to 2004 in the Nam Co basin of the Tibetan Plateau. *Chin. Sci. Bull.* **2010**, *55*, 1294–1303. [CrossRef]
25. Lei, Y.; Yao, T.; Bird, B.W.; Yang, K.; Zhai, J.; Sheng, Y. Coherent lake growth on the central Tibetan Plateau since the 1970s: Characterization and attribution. *J. Hydrol.* **2013**, *483*, 61–67. [CrossRef]
26. Tong, K.; Su, F.; Xu, B. Quantifying the contribution of glacier meltwater in the expansion of the largest lake in Tibet. *J. Geophys. Res. Atmos.* **2016**, *121*, 11158–11173. [CrossRef]
27. Zhou, J.; Wang, L.; Zhang, Y.; Guo, Y.; Li, X.; Liu, W. Exploring the water storage changes in the largest lake (Selin Co) over the Tibetan Plateau during 2003–2012 from a basin-wide hydrological modeling. *Water Resour. Res.* **2015**, *51*, 8060–8086. [CrossRef]

28. Chen, F.; Xu, Q.; Chen, J.; Birks HJ, B.; Liu, J.; Zhang, S.; Rao, Z. East Asian summer monsoon precipitation variability since the last deglaciation. *Sci. Rep.* **2015**, *5*, 11186. [CrossRef]
29. Zhang, L.; Su, F.; Yang, D.; Hao, Z.; Tong, K. Discharge regime and simulation for the upstream of major rivers over Tibetan Plateau. *J. Geophys. Res. Atmos.* **2013**, *118*, 8500–8518. [CrossRef]
30. Tian, Y.; Zhang, X.; Sun, R. Extracting alpine lake information based on multi-source and multi-temporal satellite images and its uncertainty analysis—A case study in Yamzho Yumco Basin, South Tibet. *J. Glaciol. Geocryol.* **2012**, *34*, 563–572.
31. Li, L.; Li, J.; Yao, X.; Luo, J.; Huang, Y.; Feng, Y. Changes of the three holy lakes in recent years and quantitative analysis of the influencing factors. *Quat. Int.* **2014**, *349*, 339–345. [CrossRef]
32. Song, C.; Ye, Q.; Sheng, Y.; Gong, T. Combined ICESat and CryoSat-2 altimetry for accessing water level dynamics of Tibetan lakes over 2003–2014. *Water* **2015**, *7*, 4685–4700. [CrossRef]
33. Song, C.; Huang, B.; Ke, L.; Ye, Q. Precipitation variability in High Mountain Asia from multiple datasets and implication for water balance analysis in large lake basins. *Glob. Planet. Change* **2016**, *145*, 20–29. [CrossRef]
34. Ye, Q.; Zhu, L.; Zheng, H.; Naruse, R.; Zhang, X.; Kang, S. Glacier and lake variations in the Yamzhog Yumco basin, southern Tibetan Plateau, from 1980 to 2000 using remote-sensing and GIS technologies. *J. Glaciol.* **2007**, *53*, 673–676. [CrossRef]
35. Chen, X.; Yu, Z.; Huang, Q.; Yi, P.; Shi, X.; Aldahan, A.; Chen, P. Evaluating the Water Level Variation of a High-Altitude Lake in Response to Environmental Changes on the Southern Tibetan Plateau. *J. Hydrol. Eng.* **2021**, *26*, 05021010. [CrossRef]
36. Sun, F.; Ma, R.; He, B.; Zhao, X.; Zeng, Y.; Zhang, S.; Tang, S. Changing Patterns of Lakes on The Southern Tibetan Plateau Based on Multi-Source Satellite Data. *Remote Sens.* **2020**, *12*, 3450. [CrossRef]
37. Sang, Y.F.; Chen, D.; Gong, T. What caused the decline of water level of Yamzho Yumco during 1975–2012 in the southern Tibetan Plateau? *J. Geophys. Res. Atmos.* **2020**, *125*, e2019JD031121. [CrossRef]
38. Hock, R. A distributed temperature-index ice-and snowmelt model including potential direct solar radiation. *J. Glaciol.* **1999**, *45*, 101–111. [CrossRef]
39. Lundquist, J.; Hughes, M.; Gutmann, E.; Kapnick, S. Our skill in modeling mountain rain and snow is bypassing the skill of our observational networks. *Bull. Am. Meteorol. Soc.* **2019**, *100*, 2473–2490. [CrossRef]
40. Immerzeel, W.W.; Petersen, L.; Ragettli, S.; Pellicciotti, F. The importance of observed gradients of air temperature and precipitation for modeling runoff from a glacierized watershed in the Nepalese Himalayas. *Water Resour. Res.* **2014**, *50*, 2212–2226. [CrossRef]
41. Zeng, C.; Zhang, F.; Wang, L.; Chen, D. Summer precipitation characteristics on the southern Tibetan plateau. *Int. J. Climatol.* **2021**, *41*, E3160–E3177. [CrossRef]
42. Goodarzi, M.R.; Pooladi, R.; Niazkar, M. Evaluation of Satellite-Based and Reanalysis Precipitation Datasets with Gauge-Observed Data over Haraz-Gharehsoo Basin, Iran. *Sustainability* **2022**, *14*, 13051. [CrossRef]
43. Wang, X.; Tolksdorf, V.; Otto, M.; Scherer, D. WRF-based dynamical downscaling of ERA5 reanalysis data for High Mountain Asia: Towards a new version of the High Asia Refined analysis. *Int. J. Climatol.* **2021**, *41*, 743–762. [CrossRef]
44. Jiang, Y.; Yang, K.; Li, X.; Zhang, W.; Shen, Y.; Chen, Y.; Li, X. Atmospheric simulation-based precipitation datasets outperform satellite-based products in closing basin-wide water budget in the eastern Tibetan Plateau. *Int. J. Climatol.* **2022**, *42*, 1–17. [CrossRef]
45. Li, D.; Yang, K.; Tang, W.; Li, X.; Zhou, X.; Guo, D. Characterizing precipitation in high altitudes of the western Tibetan plateau with a focus on major glacier areas. *Int. J. Climatol.* **2020**, *40*, 5114–5127. [CrossRef]
46. Sun, H.; Su, F. Evaluation of multiple precipitation datasets and their potential utilities in hydrologic modeling over the Yarlung Zangbo River Basin. *Prog. Geogr.* **2020**, *39*, 1126–1139. [CrossRef]
47. Sun, R.; Zhang, X.; Sun, Y.; Zheng, D.; Fraedrich, K. SWAT-based streamflow estimation and its responses to climate change in the Kadongjia river watershed, southern Tibet. *J. Hydrometeorol.* **2013**, *14*, 1571–1586. [CrossRef]
48. Wang, L.; Zhang, F.; Zhang, H.; Scott, C.A.; Zeng, C.; Shi, X. Intensive precipitation observation greatly improves hydrological modelling of the poorly gauged high mountain Mabengnong catchment in the Tibetan Plateau. *J. Hydrol.* **2018**, *556*, 500–509. [CrossRef]
49. Yang, D.; Kane, D.; Zhang, Z.; Legates, D.; Goodison, B. Bias corrections of long-term (1973–2004) daily precipitation data over the northern regions. *Geophys. Res. Lett.* **2005**, *32*, 312–321. [CrossRef]
50. Li, Z.; Shi, X.; Tang, Q.; Zhang, Y.; Gao, H.; Pan, X.; Stephen, J.D.; Zhou, P. Partitioning the contributions of glacier melt and precipitation to the 1971–2010 runoff increases in a headwater basin of the Tarim River. *J. Hydrol.* **2020**, *583*, 124579. [CrossRef]
51. Wu, L.; Zhang, X.; Hao, F.; Wu, Y.; Li, C.; Xu, Y. Evaluating the contributions of climate change and human activities to runoff in typical semi-arid area, China. *J. Hydrol.* **2020**, *590*, 125555. [CrossRef]
52. Bontemps, S.; Defourny, P.; Van Bogaert, E.; Team ES, A.; Arino, O.; Kalogirou, V.; Perez, J.R. *GLOBCOVER 2009 Products Description and Validation Report*; UCLouvain: Louvain, Belgium; ESA: Darmstadt, Germany, 2009.
53. Nachtergaele, F.; Van, V.H.; Verelst, L.; Batjes, N.; Dijkshoorn, K.; Van, E.V.; Shi, X. *Harmonized World Soil Database*; Version, 1.1; FAO: Rome, Italy; IIASA: Laxenburg, Austria, 2009.
54. Hao, X. *Long Time Series Data of Snow Cover Area on Qinghai-Tibet Plateau (2003–2014)*; National Tibetan Plateau Data Center: Beijing, China, 2019.
55. Maussion, F.; Scherer, D.; Mölg, T.; Collier, E.; Curio, J.; Finkelnburg, R. Precipitation seasonality and variability over the Tibetan Plateau as resolved by the High Asia Reanalysis. *J. Clim.* **2014**, *27*, 1910–1927. [CrossRef]

56. Tarasova, L.; Knoche, M.; Dietrich, J.; Merz, R. Effects of input discretization, model complexity, and calibration strategy on model performance in a data-scarce glacierized catchment in Central Asia. *Water Resour. Res.* **2016**, *52*, 4674–4699. [CrossRef]
57. Kralisch, S.; Krause, P. JAMS-a Framework for Natural Resource Model Development and Application. In Proceedings of the iEMSs third biannual meeting "Summit on Environmental Modelling and Software", Burlington, VT, USA, 9–13 July 2006.
58. Kralisch, S.; Krause, P.; Fink, M.; Fischer, C.; Flügel, W.A. Component based environmental modelling using the JAMS framework. In Proceedings of the MODSIM 2007 International Congress on Modelling and Simulation, Christchurch, New Zealand, 10 December 2007.
59. Flügel, W.A. Delineating hydrological units (HRU's) by GIS analysis for regional hydrological modelling using PRMS/MMS in the drainage basin of the River Broel, Germany. *Hydrol. Process.* **1995**, *9*, 423–436. [CrossRef]
60. Nepal, S. Impacts of climate change on the hydrological regime of the Koshi river basin in the Himalayan region. *J. Hydro-Environ. Res.* **2016**, *10*, 76–89. [CrossRef]
61. Nepal, S.; Flügel, W.A.; Krause, P.; Fink, M.; Fischer, C. Assessment of spatial transferability of process-based hydrological model parameters in two neighbouring catchments in the Himalayan Region. *Hydrol. Process.* **2017**, *31*, 2812–2826. [CrossRef]
62. Nepal, S.; Krause, P.; Flügel, W.A.; Fink, M.; Fischer, C. Understanding the hydrological system dynamics of a glaciated alpine catchment in the Himalayan region using the J2000 hydrological model. *Hydrol. Process.* **2014**, *28*, 1329–1344. [CrossRef]
63. Lutz, A.F.; Immerzeel, W.W.; Siderius, C.; Wijngaard, R.R.; Nepal, S.; Shrestha, A.B.; Biemans, H. South Asian agriculture increasingly dependent on meltwater and groundwater. *Nat. Clim. Change* **2022**, *12*, 455–460. [CrossRef]
64. Zhang, Y.; Luo, Y.; Sun, L.; Liu, S.; Chen, X.; Wang, X. Using glacier area ratio to quantify effects of melt water on runoff. *J. Hydrol.* **2016**, *538*, 269–277. [CrossRef]
65. Niazkar, M.; Goodarzi, M.R.; Fatehifar, A.; Abedi, M.J. Machine learning-based downscaling: Application of multi-gene genetic programming for downscaling daily temperature at Dogonbadan, Iran, under CMIP6 scenarios. *Theor. Appl. Climatol.* **2023**, *151*, 153–168. [CrossRef]
66. Jiang, Y.; Yang, K.; Yang, H.; Lu, H.; Chen, Y.; Zhou, X.; Wang, Y. Characterizing basin-scale precipitation gradients in the Third Pole region using a high-resolution atmospheric simulation-based dataset. *Hydrol. Earth Syst. Sci.* **2022**, *26*, 4587–4601. [CrossRef]
67. Henn, B.; Newman, A.J.; Livneh, B.; Daly, C.; Lundquist, J.D. An assessment of differences in gridded precipitation datasets in complex terrain. *J. Hydrol.* **2018**, *556*, 1205–1219. [CrossRef]
68. Lundquist, J.D.; Neiman, P.J.; Martner, B.; White, A.B.; Gottas, D.J.; Ralph, F.M. Rain versus snow in the Sierra Nevada, California: Comparing Doppler profiling radar and surface observations of melting level. *J. Hydrometeorol.* **2008**, *9*, 194–211. [CrossRef]
69. Moriasi, D.N.; Arnold, J.G.; Van Liew, M.W.; Bingner, R.L.; Harmel, R.D.; Veith, T.L. Model evaluation guidelines for systematic quantification of accuracy in watershed simulations. *Trans. ASABE* **2007**, *50*, 885–900. [CrossRef]
70. Zhong, Z.; Li, X.; Xu, X.; Liu, X.; He, Z. Spatial-temporal variations analysis of snow cover in China from 1992–2010. *Chin. Sci. Bull.* **2018**, *63*, 2641–2654. [CrossRef]
71. Zhang, H.; Zhang, F.; Zhang, G.; He, X.; Tian, L. Evaluation of cloud effects on air temperature estimation using MODIS LST based on ground measurements over the Tibetan Plateau. *Atmos. Chem. Phys.* **2016**, *16*, 13681–13696. [CrossRef]
72. Immerzeel, W.W.; Wanders, N.; Lutz, A.F.; Shea, J.M.; Bierkens, M. Reconciling high-altitude precipitation in the upper Indus basin with glacier mass balances and runoff. *Hydrol. Earth Syst. Sci.* **2015**, *19*, 4673–4687. [CrossRef]
73. Zhang, G.; Bolch, T.; Chen, W.; Crétaux, J.F. Comprehensive estimation of lake volume changes on the Tibetan Plateau during 1976–2019 and basin-wide glacier contribution. *Sci. Total Environ.* **2021**, *772*, 145463. [CrossRef]
74. Tan, C.; Ma, M.; Kuang, H. Spatial-temporal characteristics and climatic responses of water level fluctuations of global major lakes from 2002 to 2010. *Remote Sens.* **2017**, *9*, 150. [CrossRef]
75. Pan, Y.; Du, W.; Ma, D.; Lyu, X.; Cheng, C. Comparison of Typical Alpine Lake Surface Elevation Variations and Different Driving Forces by Remote Sensing Altimetry Method. *Int. J. Environ. Res. Public Health* **2022**, *19*, 17090. [CrossRef]
76. Vanderkelen, I.; van Lipzig, N.P.; Thiery, W. Modelling the water balance of Lake Victoria (East Africa)–part 1: Observational analysis. *Hydrol. Earth Syst. Sci.* **2018**, *22*, 5509–5525. [CrossRef]
77. Yang, X.; Wang, N.; Liang, Q.; Chen, A.A.; Wu, Y. Impacts of human activities on the variations in terrestrial water storage of the Aral Sea Basin. *Remote Sens.* **2021**, *13*, 2923. [CrossRef]
78. Tang, H.; Cida, Y.; Zeng, C.; Zhang, F. Characteristics of the lake water level changes and influencing factors in Yamzhog Yumco in Tibet from 1974 to 2019. *J. Arid. Land Resour. Environ.* **2021**, *35*, 83–89. [CrossRef]
79. You, Q.; Min, J.; Jiao, Y.; Sillanpää, M.; Kang, S. Observed trend of diurnal temperature range in the Tibetan Plateau in recent decades. *Int. J. Climatol.* **2016**, *36*, 2633–2643. [CrossRef]
80. Yang, K.; Ye, B.; Zhou, D.; Wu, B.; Foken, T.; Qin, J.; Zhou, Z. Response of hydrological cycle to recent climate changes in the Tibetan Plateau. *Clim. Change* **2011**, *109*, 517–534. [CrossRef]
81. Yang, K.; Wu, H.; Qin, J.; Lin, C.; Tang, W.; Chen, Y. Recent climate changes over the Tibetan Plateau and their impacts on energy and water cycle: A review. *Glob. Planet. Change* **2014**, *112*, 79–91. [CrossRef]
82. Yao, T.; Xue, Y.; Chen, D.; Chen, F.; Thompson, L.; Cui, P.; Toshio, K.; Lau, W.; Lettenmaier, D.; Mosbrugger, V.; et al. Recent third pole's rapid warming accompanies cryospheric melt and water cycle intensification and interactions between monsoon and environment: Multidisciplinary approach with observations, modeling, and analysis. *Bull. Am. Meteorol. Soc.* **2019**, *100*, 423–444. [CrossRef]

83. Chu, D.; Qiong, P.U.; Dui, W. Water level variations of Yamzho Yumco Lake in Tibet and the main driving forces. *J. Mt. Sci.* **2012**, *30*, 239–247.
84. Chu, D.; Pu, Q.; Laba, Z.; Zhu, L.; Zhang, X.; Pubu, C.; Deji, Y.; Sun, R. Remote sensing analysis on lake area variations of Yamzho Yumco in Tibetan Plateau over the past 40a. *J. Lake Sci.* **2012**, *24*, 494–502. [CrossRef]
85. Duethmann, D.; Bolch, T.; Farinotti, D.; Kriegel, D.; Vorogushyn, S.; Merz, B.; Pieczonka, T.; Jiang, T.; Su, B.; Güntner, A. Attribution of streamflow trends in snow and glacier melt-dominated catchments of the Tarim River, Central Asia. *Water Resour. Res.* **2015**, *51*, 4727–4750. [CrossRef]
86. Li, Z.; Li, Q.; Wang, J.; Feng, Y.; Shao, Q. Impacts of projected climate change on runoff in upper reach of Heihe River basin using climate elasticity method and GCMs. *Sci. Total Environ.* **2020**, *716*, 137072. [CrossRef] [PubMed]
87. Zhang, S.; Hua, D.; Meng, X.; Zhang, Y. Climate change and its driving effect on the runoff in the "Three-River Headwaters" region. *J. Geogr. Sci.* **2011**, *21*, s11442-s011. [CrossRef]